Drivers of an epic radiation: the role of climate and islands in species diversification and reproductive-mode evolution of Old-World tree frogs

Gajaba Ellepola[1,2], Marcio R. Pie[3], Rohan Pethiyagoda[4], James Hanken[5], Madhava Meegaskumbura[1]*

[1] College of Forestry, Guangxi Key Lab for Forest Ecology and Conservation, Guangxi University, Nanning 530004, PR China

[2] Department of Zoology, Faculty of Science, University of Peradeniya, Peradeniya, Sri Lanka

[3] Departamento de Zoologia, Universidade Federal do Paraná, Curitiba, Paraná, Brazil 81531-980

[4] Ichthyology Section, Australian Museum, Sydney, NSW 2010, Australia

[5]Museum of Comparative Zoology, Harvard University, Cambridge, MA 02138, USA

*Corresponding author

Email: madhava_m@mac.com (MM)

Key Words – Niche Evolution, Niche Conservatism, Dispersal, Refugia, Phylogenetic Diversity, Species Pumps, Climatic Correlates, Diversification Rates

Abstract

Although large diversifications of species occur unevenly across space and evolutionary lineages, the relative importance of their driving mechanisms, such as climate, ecological opportunity and key innovations, remains poorly understood. Here, we explore the remarkable diversification of rhacophorid frogs, which represent six percent of global amphibian diversity, utilize four distinct reproductive modes, and span a climatically variable area across mainland Asia, associated continental islands, and Africa. Using a complete species-level phylogeny, we find near-constant diversification rates but a highly uneven distribution of species richness. Montane regions on islands and some mainland regions have higher phylogenetic diversity and unique assemblages of taxa; we identify these as cool-wet refugia. Starting from a centre of origin, rhacophorids reached these distant refugia by adapting to new climatic conditions ('niche evolution'-dominant), especially following the origin of key innovations such as terrestrial reproduction (in the Late Eocene) or by dispersal during periods of favourable climate ('niche conservatism'-dominant).

Introduction

Since Darwin, understanding the processes underlying large-scale diversifications, wherein large assemblages of closely related lineages evolve from a common ancestor, have inspired evolutionary analyses[1–4]. Although several factors may mediate diversification, including geography, ecological opportunity, and key innovations[5], the role of the ecological niche, particularly its climatic axes, remains poorly understood[6–9].

Two main processes are central to understanding the role of climatic niche in the evolution of geographical distributions: niche conservatism (NC), where species tend to maintain their ancestral climatic niche over time[10-13]; and niche evolution (NE), where

species adapt to new climatic conditions[7-9]. To colonize climatically similar areas when NC predominates, a species requires optimal climatic conditions to move across erstwhile climatic barriers[14], whereas if NE predominates, species adapting to new conditions can overcome such barriers. Hence, knowledge of how climatic niches change over evolutionary timescales can enhance our understanding of the current distribution of lineages[8].

Rhacophorid tree frogs comprise a spectacular diversification that can be used to test climatic correlates of evolution. Encompassing nearly 6% of global anuran (frog and toad) diversity, with 432 species in 22 genera[15,16], rhacophorids occupy a large and climatically variable geographic area, mainly in Asia but with a single clade in Africa[15-18]. Across this range, rhacophorids are dispersed in distinct biogeographic regions[17,18], which include swaths of continental mainland (East/Southeast Asia, peninsular India and Africa), continental islands (Japan, Taiwan, Hong Kong, Hainan, Sri Lanka and Andaman Islands), archipelagos (Sundaland, the Philippines), and montane regions (Himalaya). The northeastern region of the subtropical-temperate Asian mainland and islands holds the early-emerging genera, which are thought to have evolved 68–53 mya[17].

Rhacophorid diversity is clustered spatially and temporally[17–20]. Some regions have greater clade or genus-level diversity (i.e., higher-level diversity), while others have high species diversity. Yet others are depauperate in both. Areas of high species diversity are often regarded as sources of diversification (species pumps), which nourish adjacent areas with lineages that evolved *in situ*[21]. However, regions with high diversification rates[22] are not always those with high phylogenetic diversity, because species diversification may occur within just one or only a few clades or genera. Although highly diverse regions exhibit distinctive as well as shared climatic characteristics, the processes that mediate rhacophorid diversification, and especially the role of climate, remain poorly known.

Understanding of this is made more complicated, however, by rhacophorids being reproductively diverse, exhibiting four distinct modes: aquatic breeding (AQ; gel-covered aquatic eggs and aquatic tadpoles), gel nesting (GN; gel-covered terrestrial eggs and aquatic tadpoles), foam nesting (FN; foam-covered terrestrial eggs and aquatic tadpoles) and direct development (DD; terrestrial eggs and froglets fully developed at hatching)[18,19,23]. The likely ancestral mode of nearly all currently recognized genera (except the basal, fully aquatic forms) is gel nesting, while DD and FN appear to be key innovations that enabled rapid diversification[19]. Because geographic ranges of some genera exhibiting the latter two reproductive modes (FN, DD) do not overlap, each mode may represent an evolutionary response to variable climatic conditions in the past. However, the climatic correlates of these reproductive modes are poorly understood and some of them may represent adaptations to spread across climatic barriers (in the context of NE).

Diversification of ectothermic tetrapods, such as anurans, is influenced by climate[24]. Since rhacophorids are distributed across a climatically variable range, and given that their diversity is clustered in space and time[17,18], we hypothesize that their diversification and dispersal has a strong climatic context (NE vs. NC), which is also associated with reproductive mode evolution. This hypothesis generates several predictions: (1) Rhacophorid diversity is clustered in climatically similar regions. A clade-level analysis should show the extent to which derived clades have shifted from the climatic niches of early-emerging clades as well as the role of NE vs. NC for each clade. (2) Regions with relatively high diversification rates such as islands and archipelagos have increased ecological opportunity, and are characterized by reproductive modes regarded as key innovations (DD and FN). (3) NE is achieved through reproductive mode evolution if correlated with specific climatic events. Analysis of this prediction will identify reproductive modes that enabled dispersal and

97 diversification into optimal climatic oases such as islands and regions that are geographically
98 disjunct from the centre of origin.
99
100 **Results and discussion**
101 We constructed an updated phylogeny of the Rhacophoridae by including 415 extant
102 species representing all 22 valid genera (Fig. 1). This represents the most complete taxon
103 sampling of rhacophorids used to date, which enhances the accuracy and support for
104 hypotheses testing of evolutionary relationships[25]. Our tree is congruent with many recent
105 clade-level analyses (Supplementary Table 1); it offers relatively high support for most major
106 nodes. It also resolves several long-standing taxonomic discordances within Rhacophoridae[18].
107 *Buergeria*, *Liuixalus*, *Theloderma* and *Nyctixalus* constitute early diverging lineages, while
108 the remaining genera diverge into two major clades: clade A—*Beddomixalus*, *Gracixalus*,
109 *Kurixalus*, *Mercurana*, *Nasutixalus*, *Philautus*, *Pseudophilautus* and *Raorchestes*; and clade
110 B—*Chirixalus*, *Chiromantis*, *Feihyla*, *Ghatixalus*, *Leptomantis, Polypedates*, *Rhacophorus,*
111 *Rohanixalus, Taruga* and *Zhangixalus.* Clade A is distributed largely across East and
112 Southeast Asia, Sundaland and the Indian subcontinent, whereas clade B is distributed largely
113 across East and Southeast Asia, Sundaland and Africa (Fig. 1).
114 Rhacophorid diversity is clustered spatially and temporally. Islands and some
115 mainland regions have higher diversity and unique assemblages of taxa (Fig. 2a). In
116 particular, species richness (SR) and phylogenetic diversity (PD) are highest in (1) montane
117 and lowland rainforest areas of Borneo; (2) rainforest areas of peninsular Malaysia; (3)
118 rainforest areas in the southern and northern Annamites of Vietnam; (4) northern Indochinese
119 subtropical forests around Yunnan; (5) northern and southern montane rainforests of the
120 Western Ghats in India; and (6) montane and lowland rainforests of Sri Lanka. These regions
121 record more than 15 species per 1°×1° global grid cell (Fig. 2a). High correlations between

SR and PD within these regions highlights their importance as species pumps and refugia for the family as a whole (Supplementary Fig. 1). Indeed, these regions are widely recognized as global centres of biodiversity[26–28], especially amphibian diversity[29,30].

The effect of climate on diversification is mediated by other factors such as the range of ecological opportunities and the particular lineages present at a given location, and thus has a strong geographic context[31]. However, geography alone cannot discern the role of climate, as similar climatic conditions may occur at different locations at different time periods and affect the evolution of independent lineages. Therefore, to understand patterns of occupation of climatic niche space and understand the climatic conditions under which rhacophorid species evolved, we extracted the mean climatic conditions of 3846 georeferenced coordinates of collecting localities of all species using data for 19 bioclimatic variables from WORLDCLIM 2.0[32]. We then used the average bioclimatic conditions in a principal component analysis (PCA) based on their correlation matrix, assuming that calculated species means reasonably approximate the realized climatic niche of a given species[9,33].

The most important dimension of the rhacophorid climatic niche (Supplementary Table 2) is dominated by variation in temperature (PC1), particularly during the cold season (BIO-6), followed by mean temperature of the warmest quarter (BIO-10) and precipitation seasonality (BIO-15). Species from regions with the greatest SR and PD primarily occupy a realized climatic niche with cool-wet conditions (Fig. 3). Such conditions, marked by mild temperatures and humid climates, are prevalent in mainland (e.g., subtropical China) and mountainous regions in tropical islands characterized by monsoonal climates[34]. In short, rhacophorid diversity is clustered in climatically similar but geographically dissimilar regions (Figs. 2a, 3). As these areas are characterized by high PD[35] as well, they also may have acted as refugia during rhacophorid diversification.

Diversification rates (DR) overlain on the phylogeny show localized variation, especially in relation to clades: rates are low in phylogenetically isolated lineages resulting from early speciation events (i.e., basal lineages), whereas high rates are associated with members of terminal diverse lineages that originated from more recent speciation events (Fig. 1). We scored and ranked all lineages with respect to their relative phylogenetic isolation[3] and then, based on these rankings, divided DR into quartiles in which the 1st quartile contains the oldest and least diverse lineages and the 4th quartile contains the youngest and most diverse ones (Supplementary Fig. 2). Subsequent mapping of species richness at a scale of 1°×1° for each quartile using IUCN species distribution range polygons[36,37] reveals geographic variation in lineage accumulation through space and time (Fig. 2b). Furthermore, as the metrics SR, PD, DR and species crown age (SA) are significantly correlated (Supplementary Fig. 1), the spatial analyses yield similar patterns regardless of which metric is used. Both early-diverging and more recent lineages accumulate within the same regions, in which SR and PD are high. Based on ancestral geographic range reconstructions, Li et al. (2013)[17] and Chen et al. (2020)[18] concluded that mainland Asia played a significant role in the early diversification of rhacophorids and that ancestors of all early lineages in the Himalaya, peninsular India, Africa and Sundaland arrived via dispersal from mainland Asia, mostly in the Oligocene. Their conclusion is supported by our finding that species richness of older lineages is highest in East/Southeast Asia. We further suggest, given the high PD in these regions, that they might also have acted as refuges for Rhacophoridae, especially during early phases of its evolutionary history.

Reconstruction of variation in speciation rate (DR statistic) onto the maximum clade credibility tree shows that rates have been approximately constant throughout rhacophorid history, with only a few instances of rate increase or decrease towards the Miocene. This pattern is confirmed by the LTT plot based on 1000 post-burnin trees (Fig. 1).

If climatic conditions within East/Southeast Asia were favourable during the period of origin of the Rhacophoridae, then one might instead expect to see an early burst of diversification[18,38]. We therefore suggest that early climates were less favourable for diversification of these frogs. This is supported by the fact that the common ancestor of the Asian tree frogs likely arrived from Madagascar around 60–70 mya possibly via the Indian plate[17] (geological evidence for early India-Asia contact is still lacking), during a relatively warmer, climatically less favourable period[39]. However, assuming that the climatic conditions in which a species occurs reflects the conditions under which it evolved (viz., if NC predominated during early stages), rhacophorids appear to have survived in cool-wet, humid subtropical climates[40], mostly towards the northeastern periphery of the family's contemporary distribution. Moreover, as most early lineages occur in close proximity to their regions of origin (cool-wet climates), we infer that NC played a major role in early diversification (Fig. 2b; Q1). This claim is corroborated by the fact that the most recent common ancestor (MRCA) and older lineages of Rhacophoridae were aquatic breeders (AQ) [18,19], a life history mode which, in rhacophorids, depends on humid and cool climatic conditions.

Ecological opportunity would have been a significant factor enabling early dispersion and diversification of rhacophorids following their arrival on the Asian plate. Indeed, they dispersed extensively from their region of origin to other parts of Asia, India, Africa and Himalaya, as well as subtropical and tropical continental islands such as Taiwan, Japan, Sundaland, Philippines and Sri Lanka[18] during phases of lowered sea level. Areas with low species richness of old lineages in the 1st quartile (Fig. 2b) may have experienced extinctions and/or immigration of lineages that had already diversified elsewhere. The distinct increase in diversifications within the same regions of origin in the 2nd quartile reaffirms the idea that NC was dominant during early dispersal and diversification.

Distribution-range expansion suggests that rhacophorids dispersed widely from their region of origin (North/Northeast Asia marked by cool-wet climates[40]) to adjacent regions during favourable climatic conditions for dispersal in the second and fourth quartiles of their diversification (Fig. 2b). Such climates have prevailed mainly during the Eocene-Oligocene transition (23–33 mya) and late Miocene (5.3–11.6 mya), during which time periodic glaciation led to depressed sea levels and the emergence of land bridges[39,41], or when lowland dry zones became colder, enabling long distance dispersal of rhacophorids, followed by subsequent diversification[38,42]. Dispersals associated with niche conservatism might have been further facilitated by increased rainfall associated with the staged, rapid rise of the Himalaya and consequent strengthening of the Asian monsoonal cycle[20,43-45].

Dispersal of rhacophorids from their centre of origin (cool-wet) to mainland (cooler, seasonal climates) and island refuges (warmer, less-seasonal climates; Fig. 3) requires traversing climatically harsh regions[46] (especially for dispersal to peninsular India and Africa) and/or sea passages that appear intermittently via land bridges, as in the Sundaland region and between India and Sri Lanka. These intervening areas and land bridges are usually lowland areas with warmer climates. Therefore, apart from dispersing only during favourable periods (NC), crossing such areas periodically would also require adapting to harsh climates (NE). Indeed, the groups most successful at dispersal and habitat utilization did so in association with evolution of their climatic niche. Climatic correlates of evolution using ES-sim are not statistically significant (Supplementary Table 3), but other analyses suggest that climate played a major role in species diversification. For example, higher disparities shown along PC3 (dominated by high summer temperatures) during the 1st quartile of diversification in East/Southeast Asia provide initial evidence that after the MRCA colonized this region, its descendants adapted (NE) to increasing summer temperatures (Fig. 4). The corresponding time periods coincide with the Middle Eocene Climatic Optimum

(MECO), a global warming event that occurred about 40 mya[47]. The subsequent Eocene-Oligocene transition, underscored by Oi-1 glaciation, resulted in a global cooling event[39] that brought about sea level lowstands[39,41] and facilitated dispersal of these warm-adapted MRCAs to adjacent refuges via intervening climatically harsh areas. Adaptation to warmer climatic conditions during the MECO thus might have been a major evolutionary advancement in common ancestors showing high dispersal capabilities during early stages of their diversification. Elevated rates of climatic niche evolution in species having broad distributional ranges further support this finding (Supplementary Table 4).

Variation in rates of climatic niche evolution among biogeographic regions suggests how species have evolved their climatic niches depending on their relative location (Supplementary Table 4). For example, after the Eocene-Oligocene transition, climatic conditions in East/Southeast Asia became colder with the Tibetan-Himalayan orogeny (ca. 30 mya), which, in turn, initiated monsoon cycles[43,44]. Species that continued to occupy cool-wet climates in East/Southeast Asia further adapted towards cooler climatic niches, punctuated by seasonal variation (Fig. 5). In contrast, species that dispersed towards lower latitudes, in particular, Sundaland and peninsular India, invariably had to adapt to climatic niches associated with higher temperatures to survive in warmer tropical environments.

Island formation during the Miocene[48] also played a significant role in shaping rhacophorid diversification. In general, a continental climate has characteristics associated with areas within a continental interior, unlike islands, which typically are influenced by surrounding bodies of water, and these differences may affect species composition[49]. Accumulation of a wealth of young rhacophorid lineages in island regions during the Miocene suggests the potential role of islands as species pumps for relatively young species (high SR) as well as refuges (high PD)[50,51] (Fig. 2b: Q4). In the PCA plot of climatic niche space, island species tend to be associated with intermediate (in subtropical islands) to

247 warmer temperatures (in tropical islands), while mainland species tend to be associated with
248 colder climates influenced by seasonality (Fig. 3). Islands tend to have less-seasonal climates
249 relative to mainland environments[52], which may buffer island species against the effects of a
250 changing climate.

251 Climatic stability on islands, however, need not imply optimality. Species
252 dispersing to islands may need to adapt to novel climatic niches. The higher rates of climatic
253 niche evolution for species living on both islands and mainland, compared to only island and
254 only mainland species, suggest that climatic niches evolved extensively in species that show
255 long-distance dispersal (Supplementary Table 5). Interestingly, island species are derived
256 from recent speciation events and have a mainland origin (Supplementary Fig. 3). Island
257 species have higher rates of evolution along PC1 and PC2, whereas mainland species tend to
258 have higher rates along PC3 (Supplementary Table 5). In the context of Rhacophoridae as a
259 whole, the pioneering ancestors of island clades may have been warm-adapted, low-elevation
260 forms that subsequently colonized relatively warm areas (i.e., islands), whereas mainland
261 species that remained in ancestral niches underwent further diversification *in situ*. However,
262 species that successfully colonized islands show higher rates of climatic niche evolution than
263 mainland species (Supplementary Table 5), which suggests that novel ecological
264 opportunities provided by mountains and other complex topographic features within islands
265 may facilitate their high diversity[5,38,53]. According to the theory of niche conservatism,
266 because islands are geographically and environmentally heterogeneous, species may be able
267 to maintain their optimal environment and enhance their chance of persistence simply by
268 dispersing across relatively small distances, especially on topographically complex islands[54].
269 This may explain how rhacophorids have diversified under less conducive, relatively warmer
270 and less seasonal climatic conditions on islands, by either NE, NC or both. Some of these
271 species, however, might at some point recolonize and re-establish in their continental

ancestral area if suitable environmental and ecological conditions return[38,55] (Supplementary Fig. 3).

Comparison of diversification rates associated with different reproductive modes and among regions (Fig. 6a) reveals that fully aquatic breeders (AQ) are found only in cool-wet East/Southeast Asia[19], whereas lineages that dispersed from this region to other regions tend to have more terrestrial reproductive modes (direct development, DD; and foam nesting, FN). Moreover, these terrestrial modes are associated with higher diversification rates in all regions. We suggest that a shift from a fully aquatic reproductive mode to more terrestrial modes, but especially DD and FN, facilitated the dispersal of rhacophorids from their centre of origin into optimal but distant climatic oases such as islands. This scenario is corroborated by the pattern of climatic niche occupation of the four reproductive modes: fully aquatic (AQ) and semi-aquatic (GN) species are confined to relatively cool-wet East/Southeast Asia and adjacent subtropical and temperate islands, whereas the more terrestrial modes are confined to warmer climates mostly found in tropical islands (mainly Borneo, Java, Sumatra, Philippines and Sri Lanka), which lie within the intertropical convergence zone (Fig. 6b).

After they colonized East/Southeast Asia, early emerging aquatic-breeding rhacophorids evolved new breeding strategies gel nesting, foam nesting and direct development, which are key evolutionary innovations (KEI) in the clade[18,19]. Species bearing more terrestrial reproductive modes tend to have broader climatic niches, and hence, wider climatic tolerance ranges, which is suggestive of greater dispersal capabilities. For example, rates of climatic niche evolution are higher in FN and DD, whereas the climatic niche in AQ has been more conservative (Supplementary Table 6). FN enables rhacophorids to lay large numbers of eggs in more open and drier habitats, where resistance to desiccation is essential[19]. Indeed, foam-nesters are characterized by large geographic ranges across potentially xeric and open habitats, making them excellent dispersers[19]. Terrestrial DD

297 instead allows frogs to lay eggs in a diversity of humid habitats away from bodies of water. It
298 represents a key innovation that facilitated the evolution of nearly half of all known
299 rhacophorid species[19], which occupy warmer but humid climatic conditions.

300 Traitgrams of different reproductive modes suggest that GN may have evolved in
301 association with the MECO global warming event during the early Eocene more than 40
302 mya[47] (Fig. 6c). GN, which is characterized by gel-covered, terrestrial eggs and free-living
303 aquatic tadpoles[23], can be regarded as an initial stage in the evolution of a fully terrestrial life
304 history[19]. Adoption of this reproductive mode has enabled NC-dominant dispersal of
305 rhacophorids into relatively cool-wet areas within close proximity to ancestral climatic niches
306 of AQ (Supplementary Fig. 4).

307 Traitgrams of the more terrestrial modes FN and DD suggest that they evolved after GN
308 but during the same geological period. Thus, increasing temperatures during MECO may
309 have promoted the adoption of novel modes of reproduction, which equipped rhacophorids
310 for a more terrestrial life. The subsequent Eocene-Oligocene transition, marked by depressed
311 sea levels, land bridge emergence[39,41] and cooler lowland dry zones, then enabled long-
312 distance dispersal of terrestrial-breeding (FN and DD) lineages. They were successful
313 dispersers insofar as they were able to overcome the ancestral dependence on aquatic habitats
314 while evolving climatic niches (NE) adapted to broader climatic conditions.

315 The spatial distribution of rhacophorid species is patchy, with islands and
316 some mainland regions having higher diversity and unique assemblages of taxa, which
317 contain older as well as relatively young lineages. This patchiness can be explained in the
318 context of climate, ecological opportunity and key evolutionary innovations. Regions of cool-
319 wet climate may have acted as climatic refuges (high PD regions). They are separated from
320 one another by warmer, climatically harsh low-lying regions and/or sea passages. Lineages
321 overcame these barriers in two main ways: by adapting to harsh climates (NE) or dispersing

only during favourable periods (NC). KEIs, such as shifting from a fully aquatic reproductive mode to more terrestrial modes, further facilitated the diversification and dispersal of rhacophorids through these climatically less favourable areas. Finally, ecological opportunity in the form of empty niches seem to have elevated diversification rates on islands, offsetting constraints caused by their less favourable (warmer) climatic conditions. Hence, for rhacophorid frogs, climatic refuges, ecological opportunity, key innovations, long periods of time to adapt to climatic conditions, and climatic niche evolution have combined to promote and sustain a remarkable diversification.

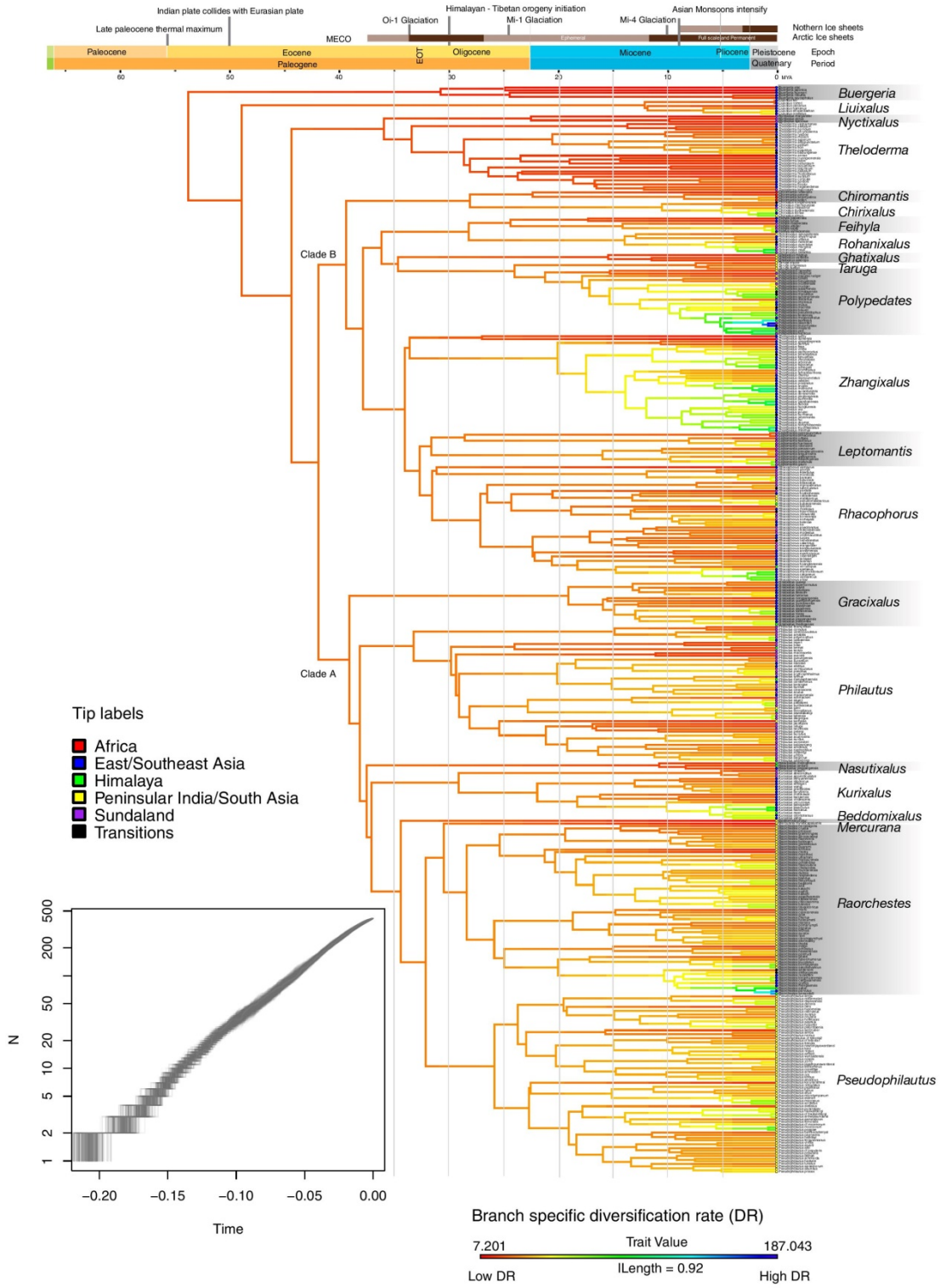

Figure 1. Complete phylogeny of rhacophorid frogs, with diversification rates (DR) traced across branches. The phylogeny is based on 58 AHE[18] and 315 Sanger sequence data for 415 species. Molecular data are unavailable for 94 species, which are constrained by assessing other taxonomic information. The lineage-through-time plot (LTT; lower left) shows a constant rate of diversification but rates traced on the phylogeny show localized variation, especially among clades (genera): younger taxa have faster diversification rates (cool colours) than older, basal taxa (warmer colours). Colored dots at branch tips indicate the geographic region in which each species occurs; "Transitions" denotes species occurring in two or more regions.

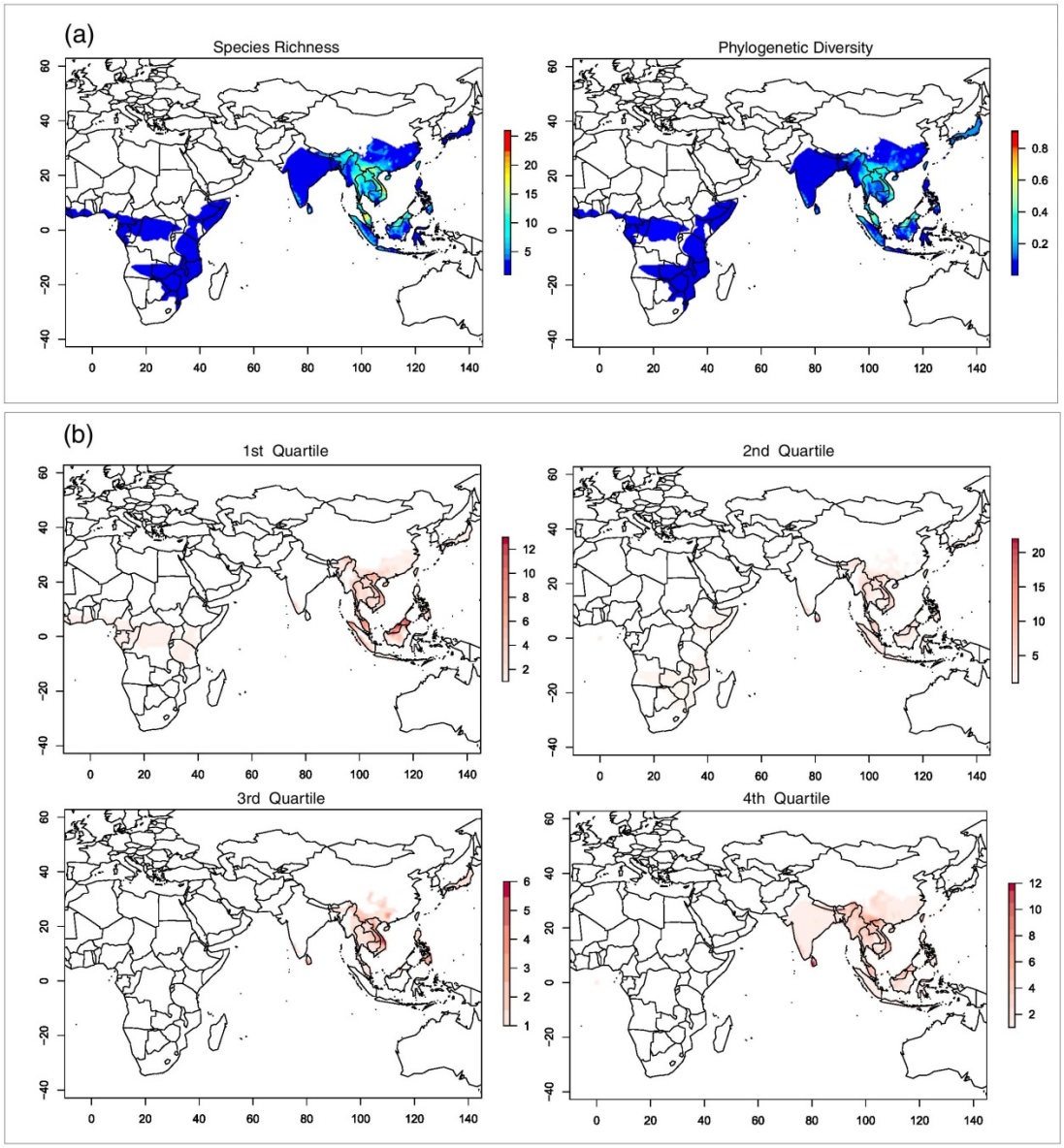

Figure 2. Patterns of spatiotemporal distribution in Rhacophoridae (a) Spatial clustering of species richness (SR) and phylogenetic diversity (PD) in 1°×1° grid cells based on presence-absence matrices derived from species' geographic ranges (see Methods). SR and PD are highest in the Sunda islands, peninsular Malaysia, Vietnam, the Yunnan-Guizhou plateau area, the Western Ghats of India and Sri Lanka. (b) Species richness in 1°×1° grid cells for each DR quartile. Dark red highlights grid cells with high species richness; light red indicates cells with low species richness within the respective DR quartile. DR values represent the number and timing of diversification events along a lineage: the 1st DR quartile represents species with low diversification rates (consisting of older lineages having few close relatives), whereas the 4th quartile represents species with faster diversification (having many young and close relatives). Highest species richness is observed during the 2nd quartile and generally in the same regions as those of 1st-quartile species, indicating early dispersal and diversification events in confined areas in East/Southeast Asia, peninsular India and the Sundaland region. Regions of high SR and PD contain both the oldest and the youngest lineages. These regions may have served as species pumps and refuges during rhacophorid diversification.

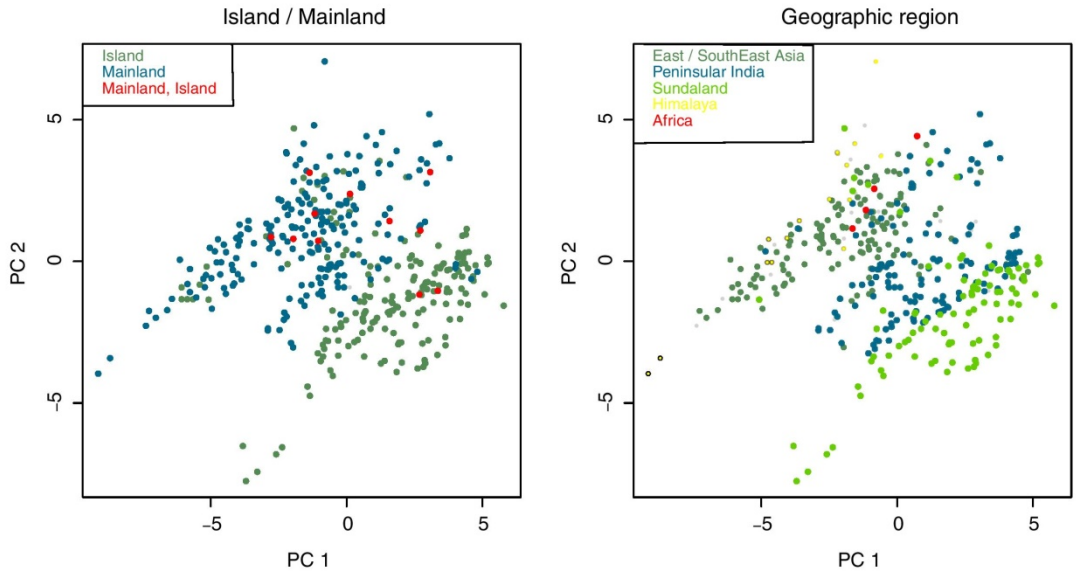

Figure 3. Climatic space defined by the first two principal component axes of climate niches in Rhacophoridae. Each point represents the average climatic conditions of a single species. Loadings are provided in Table S2. PC1 explains 40.5% of the variance and reflects variation in temperature; PC2 explains 23.9% of the variance and reflects variation in temperature and rainfall. Geographically, species in Sundaland are adapted to warm and less-seasonal climates, whereas species from East/Southeast Asia and Himalaya are cool-wet adapted. General patterns indicate that island species are comparatively warm adapted while mainland species are more or less cool-wet adapted.

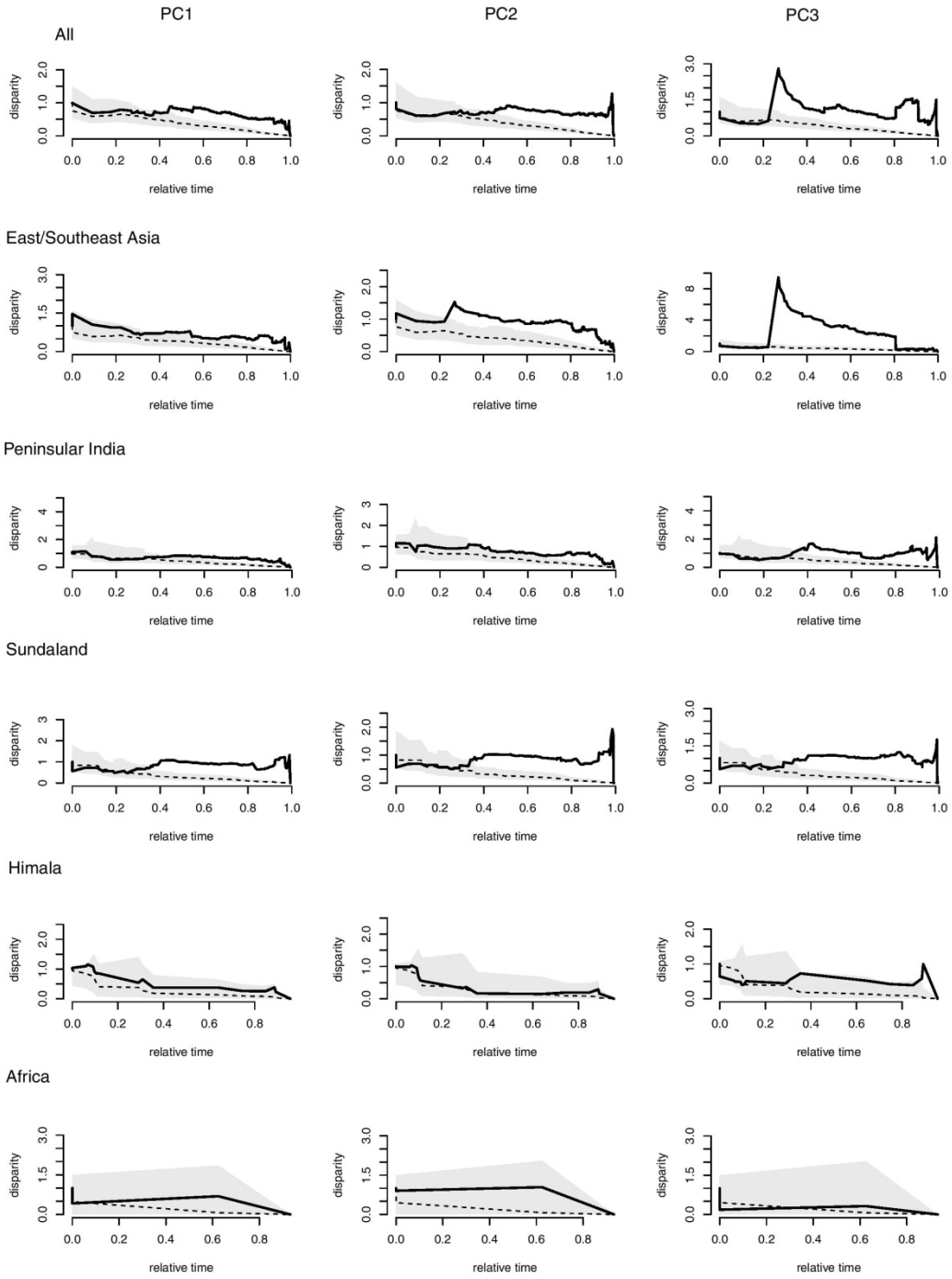

Figure 4. Relative disparity-through-time (DTT) of PC scores representing rhacophorid climatic niches. Solid lines indicate observed DTT values; dashed lines and the corresponding polygons represent the averages and 95% confidence intervals, respectively, of the expectations given a constant accumulation of disparity over time based on 999 pseudoreplicates. Disparity of climatic niche evolution is higher especially during the second half of the diversification in all biogeographic regions except Africa. Markedly higher levels of disparity are observed in PC3 (higher summer temperature) early in the evolution of species from East/Southeast Asia and peninsular India and recently in species from Sundaland.

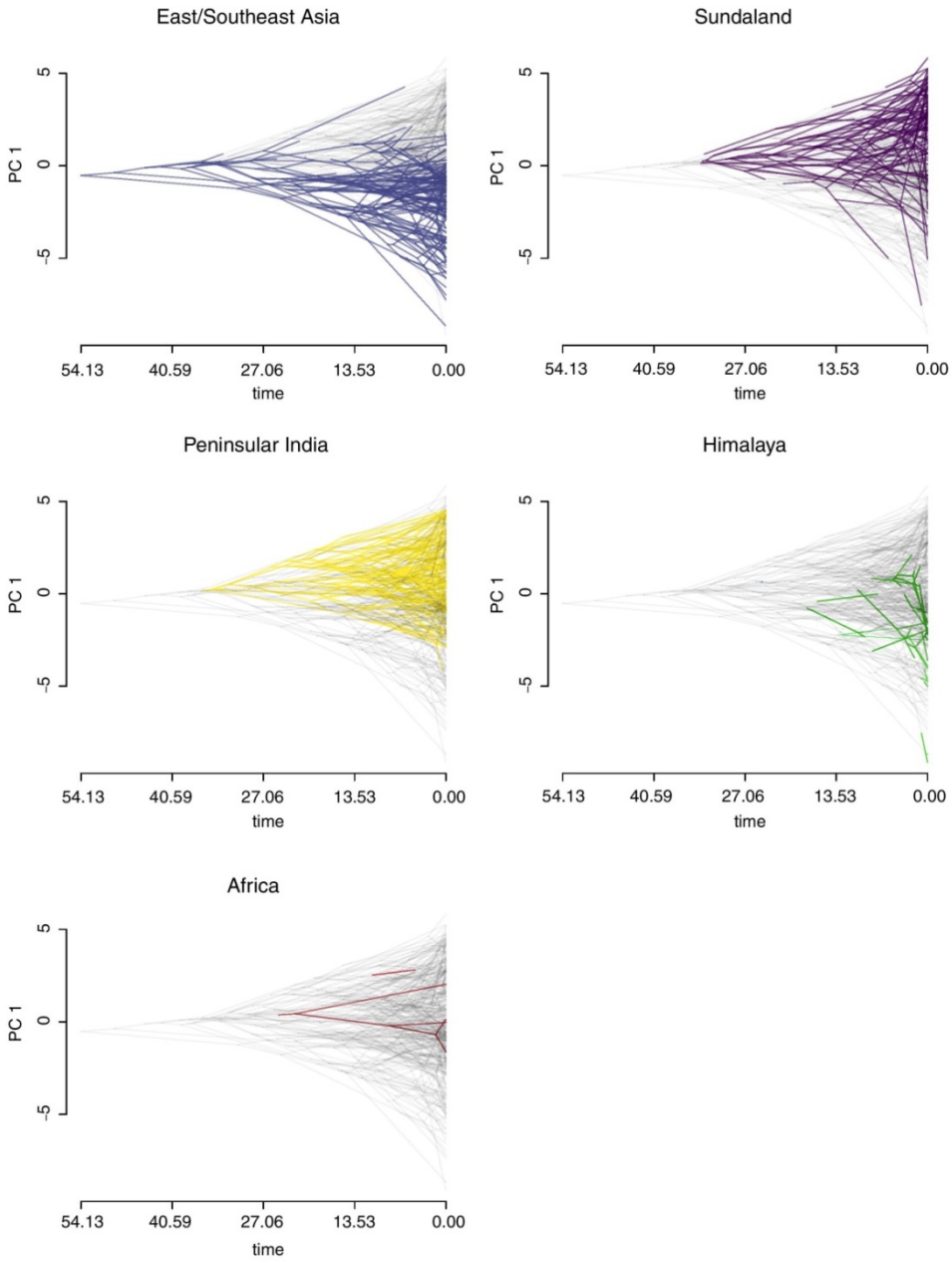

Figure 5. Variation among biogeographic regions in the rate of evolution of the climatic niche explained by the first principal component axis (PC1) of average climatic conditions for each rhacophorid species. The X-axis corresponds to the approximate age of origin of rhacophorid clades to the present (indicated by quartiles); nodes indicate the inferred climatic niches for the most recent common ancestor of the extant taxa defined by that node; positive values along Y-axis represent warmer climates whereas negative values represent colder climates; gray branches in the background of each plot indicate the overall climatic niche evolution of rhacophorids along PC 1. Divergent branches are more frequent near the present time. While species in East/Southeast Asia (blue) and Himalaya (green) have evolved towards colder climatic conditions and those in Sundaland (purple) and peninsular India (yellow) have evolved towards warmer climatic conditions, species in Africa (red) have not deviated much from their ancestral climatic niche.

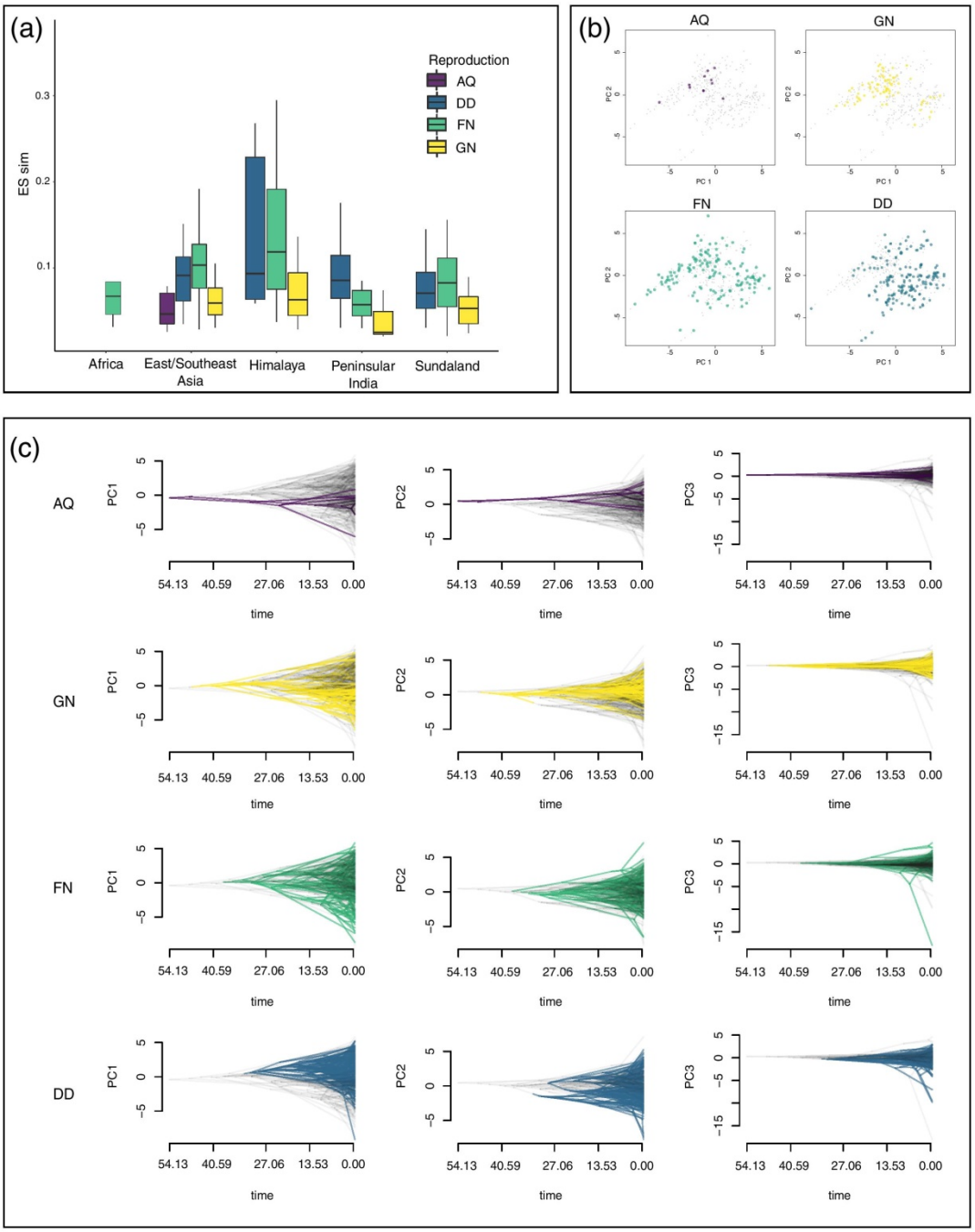

Figure 6. Climatic correlates of different rhacophorid reproductive modes. (a) Box plot showing diversification rates (DR) associated with different reproductive modes in different biogeographic regions (aquatic breeding, AQ; gel nesting, GN; foam nesting, FN; and direct development, DD). Species having FN and DD show high diversification rates. (b) PCA plots depict climatic niche occupation of species that utilize the above four reproductive modes. Aquatic breeders display a conservative (narrow) occupation of climatic niche space, whereas FN have the broadest niche. DD are restricted mostly to warmer but humid and less seasonal climates. (c) Variation in the rate of evolution of the rhacophorid climatic niche explained by the first three principal component axes (PC1–PC3) of average climatic conditions for each reproductive mode. Early AQ shows a pattern of niche conservatism whereas GN, FN and DD, which have facilitated the evolutionary transition of rhacophorids to a more terrestrial life, appear to have evolved their climatic niches during relatively warmer early Eocene (40 mya) conditions. Newly evolved reproductive modes show a pattern of

broadening their climatic niches subsequent to the Eocene-Oligocene transition (23–33 mya), which was marked by favourable climatic conditions.

Methods

Comprising 6% of global amphibian diversity, rhacophorid tree frogs occupy a climatically variable geographic area ranging from tropical and sub-tropical Asia, its continental islands and archipelagos, to Africa. We carried out a series of analyses based on a complete species phylogeny for Rhacophoridae using a combination of phylogenetic inference and phylogenetic imputation to determine how climate has shaped the diversification and dispersal of this charismatic group.

Phylogenetic inference

Extensive taxon sampling is important in phylogenetic systematics; it increases accuracy and support of evolutionary relationships[25]. Hence, we derived an updated phylogeny of the family Rhacophoridae with the most complete taxon sampling used to date: 415 extant species representing all 22 genera. Although previous studies have resolved many of the earlier controversies in rhacophorid phylogeny (Table S1), taxonomic discordances persist[18], hindering the testing of hypotheses for major evolutionary questions. Moreover, the genetic data available for different rhacophorid lineages are uneven, ranging from none for some species to whole-genome sequences for others, which leads to incomplete taxon sampling. Therefore, we took three main steps to derive a complete species-level phylogeny: (i) establish a phylogenomic backbone, (ii) compile Sanger sequence data of non-chimeric sequences, and (iii) add species without genetic data using phylogenetic imputation[56]. We began by reanalysing the anchored hybrid enrichment dataset (AHE) of Chen et al. (2020)[18]. Although there was strong support for most branches of the rhacophorid tree, one clade (comprised of *Pseudophilautus*, *Kurixalus* and *Raorchestes*) proved recalcitrant; it was unstable in species-tree analyses. We estimated Maximum Likelihood trees for each locus

using RAxML 8.2.12[57]; branch support for each gene tree was based on 50 bootstrap replicates. Preliminary analyses indicated that the source of instability was the position of *Nasutixalus*, given that a species tree without that terminal using ASTRAL III v.5.7.3[58] yielded 100% local posterior probabilities for the relationship among *Pseudophilautus*, *Kurixalus* and *Raorchestes*. We therefore enumerated the loci that supported each of the three alternative topologies, as well as the corresponding average bootstrap values of the loci supporting each of them. Given that one of the alternative topologies tended to be more strongly supported by loci with higher average bootstraps (Fig. S5), that topology was chosen for downstream analyses.

Once a stable backbone tree was obtained, we compiled all Sanger sequence data available from GenBank (last accessed January 2021), which included 315 rhacophorid species (number of species/genus in parentheses): *Beddomixalus* (1), *Buergeria* (3), *Chirixalus* (2) *Chiromantis* (3), *Feihyla* (4), *Ghatixalus* (3), *Gracixalus* (9), *Kurixalus* (17), *Leptomantis* (10), *Liuixalus* (6), *Mercurana* (1), *Nasutixalus* (3), *Nyctixalus* (3), *Philautus* (31), *Polypedates* (14), *Pseudophilautus* (56), *Raorchestes* (59), *Rhacophorus* (32), *Rohanixalus* (2), *Taruga* (3), *Theloderma* (25) and *Zhangixalus* (28; see supplementary material, Table S7). Sequences were obtained for seven gene fragments: mitochondrial loci 16S, 12S and *cyt-b*; and nuclear loci *BDNF, Rag-1, rhod* and *Tyr*. Each locus was aligned separately using MUSCLE[59] as implemented in MEGA v.6[60]. Sequences of all fragments were then concatenated, with a total alignment length of 3923 base pairs (bp).

We obtained complete species-level trees by using the two-stage Bayesian approach PASTIS[56]. This method uses as inputs a backbone topology based on molecular data, a set of taxonomic postulates (e.g., constraining species to belong to specific genera or families) and user-defined priors on branch lengths and topologies. Based on these inputs, PASTIS produces input files for MrBayes 3.2.5[61], which generates a posterior distribution of

complete ultrametric trees that capture uncertainty under a homogeneous birth-death prior model of diversification and placement constraints. We used PASTIS version 0.1-2, with functions from the APE 5.4[62]and CAPER 0.2[63] packages. There are two main assumptions to this approach: (i) taxonomic groups (e.g., genera) are monophyletic unless there is evidence (i.e., genetic data) that suggests otherwise; and (ii) reasonable edge-length and topology priors (i.e., birth-death models) exist. PASTIS has been used to provide large-scale trees of several higher-level taxa, including birds[64], squamates[65], and sigmodontine rodents[66]. Thomas et al. (2013)[56] categorize species into three types: type 1 species have genetic information (i.e., genomic data + Sanger sequencing data); type 2 species lack genetic information but are congeners of a species with genetic information; and type 3 species lack genetic data and are members of a genus that lacks genetic data. In our dataset we have 321 (genetic data present) and 94 (genetic data absent; Figure S6) species exclusively from types 1 and 2, respectively. Our backbone tree was established using the anchored hybrid enrichment dataset[18]. Species without genetic data are constrained to their closest relatives based on morphology as indicated in published literature (Table S8) and the best partitioning scheme for the Sanger dataset was determined using PartitionFinder2[67]. The general time-reversible model with an invariable gamma rate for each partition, birth-death as prior probability distribution on branch lengths, fixed extinction-rate priors and exponential net speciation-rate priors were assigned to the alignment and constraints was run on MrBayes 3.2.5 for 20 million generations. Convergence was assessed by inspecting the log-output file in TRACER v.1.6[68] and by ensuring ESS values were greater than 200. The first 10% of the trees were discarded, and the post burn-in trees used to infer the maximum clade credibility tree using TREEANNOTATOR v.1.10.4[69]. The maximum clade credibility tree, as well as a set of 1000 post burn-in topologies (provided in supplementary data), were retained for further analyses (see below).

To examine the temporal context of divergence and correlate it with geological and climatic events, we estimated divergence times among lineages in a separate run of the above partitioned dataset. We initially used the lognormal relaxed clock model with default clock rate priors and, subsequently, the default strict clock model. The lognormal relaxed clock model, which showed the greatest fit, was used for further analysis. We calibrated the tree using two literature-based, molecular-estimated points from Meegaskumbura et al. (2019)[38] and Chen et al. (2020)[18] (viz., the age of the MRCA of extant *Pseudophilautus*, 21.93–45.14 mya; and the age of the MRCA of clade A, 31.65–40.53 mya, respectively).

Testing for variation in rates of lineage diversification

We tested for potential correlates of speciation rates using ES-sim, a semi-parametric test for trait-dependent diversification analyses[70]. Instead of modelling the relationship between traits and diversification, ES-sim tests for correlations between summary statistics of phylogenetic branching patterns and trait variation at the tips of a phylogenetic tree. It uses the DR statistic[65], a non-model-based estimator of speciation rate that is computed for a given species, as a weighted average of the inverse branch lengths connecting the focal species to the root of the phylogeny (e.g., the root-to-tip set of branches). The use of tip-specific metrics of speciation rate may provide an alternative to parametric state-dependent diversification due to the elevated rates of false-positive results, given that heterogeneity in diversification rates of the underlying phylogeny could bias inferences of associations between traits and diversification regardless of their underlying relationship[71]. Simulations show that the use of ES-sim for continuous traits shows equal or superior power than QuaSSE[70]. In addition, given that they are computationally efficient, tip-specific metrics make it feasible to explore the impact of phylogenetic uncertainty. ES-sim was implemented using the code provided by

509 Harvey & Rabosky (2018)[70] (available at https://github.com/mgharvey/ES-sim) and we
510 initially assessed variation in speciation rates among lineages by mapping variation in the DR
511 statistic along the maximum clade credibility tree using the 'contmap' function in
512 PHYTOOLS 0.7-47[72]. Given that the DR statistic tends to focus more on processes closer to
513 the present, we compare those results with lineages-through-time (LTT) plots using 1000
514 alternative trees using the 'mltt.plot' function in APE.
515
516 *Spatio-temporal patterns of rhacophorid diversification*
517 We downloaded distribution ranges as spatial data polygons from IUCN (2020)[36]
518 http://www.iucnredlist.org/technical-documents/spatial-data for all available rhacophorid
519 species and transformed them into a presence-absence matrix (PAM) by using a 1°×1° global
520 grid using the function 'lets.presab' in R package letsR V 3.2[37]. Species richness (SR) was
521 visualized as species richness values per cell on a world map by applying the function 'plot'
522 in letsR. Using the maximum clade credibility tree, we calculated phylogenetic diversity
523 (PD), determined as the sum of all co-occurring species branch lengths[73] within each cell, by
524 applying the function 'lets.maplizer,' and obtained a raster to map geographic patterns of PD.
525 Similarly, geographic distribution maps were created for both the DR estimated above[70] and
526 species crown age (SA), estimated as the length of the terminal branch subtending each
527 species until the most recent speciation event, to visualize spatial patterns of diversification.
528 As many young (recent) lineages and close relatives attain high values of DR,
529 and those with few close relatives (older/basal lineages) yield lower values (Fig. 1), DR
530 allows us to effectively score all lineages with respect to their relative phylogenetic
531 isolation[3]. As the above metrics (SR, PD, DR and SA), especially DR and SA, are
532 significantly correlated (Fig. S1), the spatial analyses produce more or less similar patterns
533 regardless of the metric assessed. In the main text, we therefore focus on results using DR

values. Following Kennedy et al. (2017)[3], we used the species ranks of DR to divide our distributional database into quartiles. The first quartile contains the oldest and least diverse lineages, while the fourth quartile contains the youngest and most diverse ones (Figure 2B). We subsequently generated maps of species richness at the 1°×1° scale for each quartile using the 'lets.maplizer' function in the package letsR. This enables us to visualize areas that have accumulated a higher or lower number of species in each DR quartile. Alternatively, this reveals geographic variation in lineage accumulation through space and time. Moreover, relative and distinct increase in diversifications within the same regions in quartiles would support the idea of NC-dominant early dispersal and diversification. Finally, to explicitly test whether islands serve as species pumps, we used island/mainland as a binary trait and ran ES-sim on 100 potential topologies. Due to the highly correlated nature of DR and SA (Fig. S7), it can be assumed that each quartile represents the temporal aspect of diversification as well.

To further investigate species accumulation through time in different biogeographic regions (East/Southeast Asia, Sundaland, peninsular India, Himalaya and Africa), we used subsets of the rhacophorid phylogeny based on geographic region and assigned birth-death models of diversification under four conditions for the birth and death rates specified in the package RPANDA[74]. Best models were selected for each biogeographic region based on AICc values, and diversity through time was visualized using the function 'plotdtt' in RPANDA (Figure S2).

Ecological and biogeographic data

Information on geographical distribution of rhacophorid species derived from occurrence records was obtained from the GBIF database (https://www.gbif.org) using RGBIF 1.4.0[75] in R v.3.6.1[76]. Distribution data for species not represented in GBIF were obtained directly from the literature and IUCN species range maps. The final distribution dataset comprised 3846

559 geographical coordinates of all species. Nearly 65% of those species (N = 273) were
560 represented by single-occurrence records. This is not uncommon in compilations of this
561 nature[9,33] and reflects the high degree of local endemism of rhacophorid species. Information
562 on 19 bioclimatic variables for each occurrence point were obtained from WORLDCLIM
563 2.0[32] using the "extract" function in RASTER 3.0-7[77]. Mean values for each bioclimatic
564 variable for each species are provided in Table S4. We then used the average bioclimatic
565 conditions in a principal components analysis (PCA) based on their correlation matrix. The
566 axes to be retained for further analyses were determined using the broken-stick method as
567 implemented in VEGAN 2.5-6[78]. We assume that the measured species means are a
568 reasonable approximation of the realized climatic niche of the species[9,33].
569
570 *Climatic correlates of rhacophorid diversification*
571 When implementing ES-sim[70], we used 100 simulations to build the null distribution of trait-
572 speciation associations for significance testing. The designated potential correlates of
573 speciation rates were the first three principal components of the climatic niches, mean
574 elevation and whether these species were island endemics. To account for phylogenetic
575 uncertainty, we repeated each analysis for 100 potential topologies. Analyses were carried
576 out separately for each potential correlate (Table S3).
577 We assessed the extent to which species traits had accumulated over time in
578 each biogeographic region (i.e., climatic niche evolution; NE along each PC axis) by using
579 disparity-through-time (DTT) plots[79], with expected disparities calculated based on 1000
580 resamplings using the 'dtt' function in GEIGER 2.0.6.2[80] and with phenograms (projections
581 of the phylogenetic tree in a space defined by phenotype and time) using the 'phenogram'
582 function in PHYTOOLS. Biogeographic categorizations for these analyses are based on Chen
583 et al. (2020)[18]. Here, East/Southeast Asia includes mainland China and subtropical islands

584 such as Hainan, Taiwan and Japan; Sundaland includes peninsular Malaysia and islands such
585 as Borneo, Sumatra, Java and Philippines; and peninsular India includes mainland India and
586 Sri Lanka.

587 We tested whether evolutionary rates of the main climatic niche axes (PC1,
588 PC2 and PC3) differ significantly among species inhabiting different biogeographic regions,
589 islands, mainland, and both islands and mainland. We assumed that species living both on
590 islands and mainland have a broader climatic niche than only-island and only-mainland
591 species; high rates of climatic niche evolution of those species would suggest NE. We used
592 1000 potential trait histories from stochastic character mapping and then fit two alternative
593 models of evolution on each studied trait—one that fixes the rate of niche evolution to be
594 identical between island / mainland inhabitants, and an alternative model in which the
595 inhabitants have separate rates. We calculated the Akaike Information Criterion for small
596 sample size (AICc) from the maximum likelihood estimate on each tree using the
597 'brownie.lite' function in PHYTOOLS. Subsequently, we calculated model-averaged
598 estimates of evolutionary rates for each category. Similarly, rates of climatic niche evolution
599 associated with different reproductive modes were assessed using the above method.

600 Finally, to infer the biogeographic history of Rhacophoridae by determining
601 whether lineages originated on islands or on mainland, a model-testing approach was applied
602 using the R package BioGeoBEARS v.0.2.1[81] based on the maximum credibility tree. Species
603 occurrences were categorized according to the biogeographic areas modified from Chen et
604 al., 2020[18]: (1) Africa mainland; (2) peninsular India (mainland); (3) Sri Lanka (island); (4)
605 East/Southeast Asia mainland; (5) East/Southeast Asian islands, including Japan, Taiwan,
606 Hongkong and Hainan; (6) Sundaland (island archipelago); and (7) Himalaya. Given the
607 extreme geological complexity of the region through time, dispersal constraints were not

608 applied[18]. Analyses used six biogeographic models specified in the package (Table S9) and
609 model fit was assessed using the Akaike Information Criterion (AIC) and Akaike weights[81].

610
611
612
613
614

615 **References**

616 1. Purvis, A., Fritz, S. A., Rodríguez, J., Harvey, P. H. & Grenyer, R. The shape of
617 mammalian phylogeny: patterns, processes and scales. *Phil. Trans. R. Soc. B* **366**, 2462–
618 2477 (2011).
619 2. Pyron, R. A. & Wiens, J. J. Large-scale phylogenetic analyses reveal the causes of high
620 tropical amphibian diversity. *Proc. R. Soc. B* **280**, 20131622 (2013).
621 3. Kennedy, J. D. *et al.* Does the colonization of new biogeographic regions influence the
622 diversification and accumulation of clade richness among the Corvides (Aves:
623 Passeriformes)? *Evolution* **71**, 38–50 (2017).
624 4. Barahona, R. S., Sauquet, H. & Magallón, S. The delayed and geographically
625 heterogeneous diversification of flowering plant families. *Nat. Ecol. Evol.* **4**, 1232–1238
626 (2020).
627 5. Stroud, J. T. & Losos, J. B. Ecological opportunity and adaptive radiation. *Annu. Rev.*
628 *Ecol. Evol. Syst.* **47**, 507–532 (2016).
629 6. Graham, C. H., Ron, S. R., Santos, J. C., Schneider, C. J. & Moritz, C. Integrating
630 phylogenetics and environmental niche models to explore speciation mechanisms in
631 dendrobatid frogs. *Evolution* **58**, 1781–1793 (2004).
632 7. Duran, A., Meyer, A. L. S. & Pie, M. R. Climatic niche evolution in New World monkeys
633 (Platyrrhini). *PLoS ONE* **8**, e83684 (2013).
634 8. Pie, M. R. The macroevolution of climatic niches and its role in ant diversification:

635 Evolution of ant climatic niches. *Ecol. Entomol.* **41**, 301–307 (2016).

636 9. Pie, M. R., Campos, L. L. F., Meyer, A. L. S. & Duran, A. The evolution of climatic
637 niches in squamate reptiles. *Proc. R. Soc. B* **284**, 20170268 (2017).

638 10. Evans, M. E. K., Smith, S. A., Flynn, R. S. & Donoghue, M. J. Climate, niche evolution,
639 and diversification of the "Bird-Cage" evening primroses (*Oenothera*,
640 sections *Anogra* and *Kleinia*). *Amer. Nat.* **173**, 225–240 (2009).

641 11. Peterson, T. A. & Cohoon, K. P. Sensitivity of distributional prediction algorithms to
642 geographic data completeness. *Ecol. Model.* **117**, 159–164 (1999).

643 12. Wiens, J. J., & Graham, C. H. Niche conservatism: integrating evolution, ecology, and
644 conservation biology. *Annu. Rev. Ecol. Evol. Syst.* **36,** 519–539 (2005).

645 13. Wiens, J. J., Ackerly, D. D., Allen, A. P. *et al.* Niche conservatism as an emerging
646 principle in ecology and conservation biology. *Ecol. Let.* **13**, 1310–1324 (2010).

647 14. Parmesan C, & Yohe, G. A globally coherent fingerprint of climate change impacts
648 across natural systems. *Nature* **421,** 37–42 (2003).

649 15. AmphibiaWeb. *Information on amphibian biology and conservation. University of*
650 *California, Berkeley, California:* http://www.amphibiaweb.org/ (2020).

651 16. Frost, D. R. *Amphibian Species of the World. An Online Reference. Version 6.1*
652 https://amphibiansoftheworld.amnh.org/index.php (2020).

653 17. Li, J.-T. *et al.* Diversification of rhacophorid frogs provides evidence for accelerated
654 faunal exchange between India and Eurasia during the Oligocene. *Proc. Natl. Acad. Sci.*
655 *U.S.A.* **110**, 3441–3446 (2013).

656 18. Chen, J.-M. *et al.* An integrative phylogenomic approach illuminates the evolutionary
657 history of Old World tree frogs (Anura: Rhacophoridae). *Mol. Phylog. Evol.* **145**, 106724
658 (2020).

659 19. Meegaskumbura, M. *et al.* Patterns of reproductive-mode evolution in Old World tree

660 frogs (Anura, Rhacophoridae). *Zool. Scr.* **44**, 509–522 (2015).
661 20. Pan, T. *et al.* The reanalysis of biogeography of the Asian tree frog, *Rhacophorus* (Anura:
662 Rhacophoridae): geographic shifts and climatic change influenced the dispersal process
663 and diversification. *PeerJ* **5**, e3995 (2017).
664 21. Condamine, F. L., Leslie, A. B. & Antonelli, A. Ancient islands acted as refugia and
665 pumps for conifer diversity. *Cladistics* **33**, 69–92 (2017).
666 22. Becerra, J. X. & Venable, D. L. Sources and sinks of diversification and conservation
667 priorities for the Mexican tropical dry forest. *PLoS ONE* **3**, e3436 (2008).
668 23. Grosjean, S., Delorme, M., Dubois, A. & Ohler, A. Evolution of reproduction in the
669 Rhacophoridae (Amphibia, Anura). *J. Zool. Syst.* **46**, 169–176 (2008).
670 24. Rolland, J. *et al.* The impact of endothermy on the climatic niche evolution and the
671 distribution of vertebrate diversity. *Nat. Ecol. Evol.* **2**, 459–464 (2018).
672 25. Zwickl, D. J. & Hillis, D. M. Increased taxon sampling greatly reduces phylogenetic
673 error. *Syst. Biol.* **51**, 588–598 (2002).
674 26. Myers, N., Mittermeier, R. A., Mittermeier, C. G., da Fonseca, G. A. B. & Kent, J.
675 Biodiversity hotspots for conservation priorities. *Nature* **403**, 853–858 (2000).
676 27. Bain, R. *et al.* Amphibians of the Indomalayan realm. in S. N. Stuart (Ed.) *Threatened*
677 *Amphibians of the World.* Pp. 74–79 (Lynx Ediciones, 2008).
678 28. De Bruyn, M. *et al.* Borneo and Indochina are major evolutionary hotspots for Southeast
679 Asian biodiversity. *Syst. Biol.* **63**, 879–901 (2014).
680 29. Meegaskumbura, M. *et al.* Sri Lanka: An amphibian hot spot. *Science* **298**, 379–379
681 (2002).
682 30. Gorin, V. A. *et al.* A little frog leaps a long way: compounded colonizations of the Indian
683 subcontinent discovered in the tiny Oriental frog genus *Microhyla* (Amphibia:
684 Microhylidae). *PeerJ.* **8**, e9411 (2020).

685 31. Sillero, N & Barbosa, A. M. Common mistakes in ecological niche models, *Internat. J.*
686 *Geogr. Info. Sci.* **35** 1-14 (2020).
687 32. Fick, S. E. & Hijmans, R. J. WorldClim 2: new 1-km spatial resolution climate surfaces
688 for global land areas. *Int. J. Climatol.* **37**, 4302–4315 (2017).
689 33. Wiens, J. J., Kuczynski, C. A., Duellman, W. E. & Reeder, T. W. Loss and re-evolution of
690 complex life cycles in marsupial frogs: does ancestral trait reconstruction
691 mislead? *Evolution* **61**, 1886–1899 (2007).
692 34. Chen, D. & Chen, H. W. Using the Köppen classification to quantify climate variation
693 and change: An example for 1901–2010. *Envir. Devel.* **6**, 69–79 (2013).
694 35. Pugliesi, L. & Rapini, A. Tropical refuges with exceptionally high phylogenetic diversity
695 reveal contrasting phylogenetic structures. *Internat. J. Biodiv.* **2015**, 1–17 (2015).
696 36. IUCN (International Union for Conservation of Nature) 2019. Rhacophoridae. The IUCN
697 Red List of Threatened Species. Version 2020-3. http://www.iucnredlist.org. Downloaded
698 on 12 January 2021.
699 37. Vilela, B. & Villalobos, F. letsR: a new R package for data handling and analysis in
700 macroecology. *Meth. Ecol. Evol.* **6**, 1229–1234 (2015).
701 38. Meegaskumbura, M. *et al.* Diversification of shrub frogs (Rhacophoridae,
702 *Pseudophilautus*) in Sri Lanka – Timing and geographic context. *Mol. Phylog. Evol.* **132**,
703 14–24 (2019).
704 39. Zachos, J. Trends, rhythms, and aberrations in global climate 65 Ma to present. *Science*
705 **292**, 686–693 (2001).
706 40. Yao, Y.-F. *et al.* Reconstruction of paleovegetation and paleoclimate in the Early and
707 Middle Eocene, Hainan Island, China. *Clim. Change* **92**, 169–189 (2009).
708 41. Kominz, M. A. *et al.* Late Cretaceous to Miocene sea-level estimates from the New
709 Jersey and Delaware coastal plain coreholes: an error analysis. *Basin Rsch.* **20**, 211–226

(2008).

42. Vijayakumar, S. P., Menezes, R. C., Jayarajan, A. & Shanker, K. Glaciations, gradients, and geography: multiple drivers of diversification of bush frogs in the Western Ghats escarpment. *Proc. R. Soc. B* **283**, 20161011 (2016).
43. Licht, A. *et al.* Asian monsoons in a late Eocene greenhouse world. *Nature* **513**, 501–506 (2014).
44. Owen, L. A. & Dortch, J. M. Nature and timing of Quaternary glaciation in the Himalayan–Tibetan orogen. *Quat. Sci. Rev.* **88**, 14–54 (2014).
45. Spicer, R. A. *et al.* Why 'the uplift of the Tibetan Plateau' is a myth. *Natl. Sci. Rev.* **8**, nwaa091 (2021).
46. Klaus, S., Morley, R. J., Plath, M., Zhang, Y.-P. & Li, J.-T. Biotic interchange between the Indian subcontinent and mainland Asia through time. *Nat. Commun.* **7**, 12132 (2016).
47. Giorgioni, M. *et al.* Carbon cycle instability and orbital forcing during the Middle Eocene climatic optimum. *Sci. Rep.* **9**, 9357 (2019).
48. Hall, R. Sundaland and Wallacea: geology, plate tectonics and palaeogeography In D. J. Gower *et al.* (Eds) *Biotic Evolution and Environmental Change in Southeast Asia*. Cambridge University Press. Pp 33–78. (2012)
49. Snow, R. Continental climate and continentality. In J. E. Oliver (Ed.) *Encyclopedia of World Climatology*. Pp. 303–305 (Springer Netherlands, 2005). doi:10.1007/1-4020-3266-8_58.
50. Papadopoulou, A. & Knowles, L. L. Species-specific responses to island connectivity cycles: refined models for testing phylogeographic concordance across a Mediterranean Pleistocene aggregate island complex. *Mol. Ecol.* **24**, 4252–4268 (2015).
51. Condamine, F. L., Leslie, A. B. & Antonelli, A. Ancient islands acted as refugia and pumps for conifer diversity. *Cladistics* **33**, 69–92 (2017).

735 52. Weigelt, P., Jetz, W. & Kreft, H. Bioclimatic and physical characterization of the world's
736 islands. *Proc. Natl. Acad. Sci. U.S.A.* **110**, 15307–15312 (2013).
737 53. Parrott, L. Measuring ecological complexity. *Ecol. Indic.* **10**, 1069–1076 (2010).
738 54. Sandel, B. *et al.* The influence of Late Quaternary climate-change velocity on species
739 endemism. *Science* **334**, 660–664 (2011).
740 55. Strijk, J. S. *et al.* In and out of Madagascar: Dispersal to peripheral islands, insular
741 speciation and diversification of Indian Ocean daisy trees (*Psiadia*, Asteraceae). *PLoS*
742 *ONE* **7**, e42932 (2012).
743 56. Thomas, G. H. *et al.* PASTIS: an R package to facilitate phylogenetic assembly with soft
744 taxonomic inferences. *Meth. Ecol. Evol.* **4**, 1011–1017 (2013).
745 57. Stamatakis, A. RAxML version 8: a tool for phylogenetic analysis and post-analysis of
746 large phylogenies. *Bioinformatics* **30**, 1312–1313 (2014).
747 58. Zhang, C., Rabiee, M., Sayyari, E. & Mirarab, S. ASTRAL-III: polynomial time species
748 tree reconstruction from partially resolved gene trees. *BMC Bioinf.* **19**, 153 (2018).
749 59. Edgar, R. C. MUSCLE: a multiple sequence alignment method with reduced time and
750 space complexity. *BMC Bioinf.* **5**, 113 (2004).
751 60. Tamura, K., Stecher, G., Peterson, D., Filipski, A. & Kumar, S. MEGA6: Molecular
752 Evolutionary Genetics Analysis Version 6.0. *Mol. Biol. Evol.* **30**, 2725–2729 (2013).
753 61. Ronquist, F. *et al.* MrBayes 3.2: Efficient Bayesian phylogenetic inference and model
754 choice across a large model space. *Syst. Biol.* **61**, 539–542 (2012).
755 62. Paradis, E., Claude, J. & Strimmer, K. APE: Analyses of phylogenetics and evolution in
756 R language. *Bioinformatics* **20**, 289–290 (2004).
757 63. Orme, D. *et al. caper: Comparative Analyses of Phylogenetics and Evolution in R*
758 version 0.5. (2018). Available from: http://CRAN.R-project.org/package=caper
759 64. Jetz, W., Thomas, G. H., Joy, J. B., Hartmann, K. & Mooers, A. O. The global diversity

of birds in space and time. *Nature* **491**, 444–448 (2012).

65. Tonini, J. F. R., Beard, K. H., Ferreira, R. B., Jetz, W. & Pyron, R. A. Fully-sampled phylogenies of squamates reveal evolutionary patterns in threat status. *Biol. Cons.* **204**, 23–31 (2016).
66. Maestri, R. *et al.* The ecology of a continental evolutionary radiation: Is the radiation of sigmodontine rodents adaptive?: Evolutionary radiation on a continental scale. *Evolution* **71**, 610–632 (2017).
67. Lanfear, R., Frandsen, P. B., Wright, A. M., Senfeld, T. & Calcott, B. PartitionFinder 2: New methods for selecting partitioned models of evolution for molecular and morphological phylogenetic analyses. *Mol. Biol. Evol.* msw260 (2016) doi:10.1093/molbev/msw260.
68. Drummond, A. J., Suchard, M. A., Xie, D. & Rambaut, A. Bayesian phylogenetics with BEAUti and the BEAST 1.7. *Mol. Biol. Evol.* **29**, 1969–1973 (2012).
69. Rambaut, A. & Drummond, A. J. *TreeAnnotator v1.10.4. Available as part of the BEAST package ahttp://beast.bio.ed.ac.ukt* . (2013).
70. Harvey, M. G. & Rabosky, D. L. Continuous traits and speciation rates: Alternatives to state-dependent diversification models. *Meth. Ecol. Evol.* **9**, 984–993 (2018).
71. Beaulieu, J. M. & O'Meara, B. C. Detecting hidden diversification shifts in models of trait-dependent speciation and extinction. *Syst. Biol.* **65**, 583–601 (2016).
72. Revell, L. J. phytools: an R package for phylogenetic comparative biology (and other things). *Meth. Ecol. Evol.* **3**, 217–223 (2012).
73. Faith, D. P. Conservation evaluation and phylogenetic diversity. *Biol. Cons.* **61**, 1–10 (1992).
74. Morlon, H. *et al.* RPANDA: an R package for macroevolutionary analyses on phylogenetic trees. *Meth. Ecol. Evol.* **7**, 589–597 (2016).

75. Chamberlain, S. *et al. rgbif: Interface to the Global 'Biodiversity' Information Facility API*. R package version 0.9.8 (2020). Available at https://CRAN.R-project.org/package=rgbif

76. R Development Core Team. *a language and environment for statistical computing: reference index*. (R Foundation for Statistical Computing, 2010).

77. Hijmans, R. J. *et al. raster: Geographic Data Analysis and Modeling (R package)*. (2020). Available at https://CRAN.R-project.org/package=raster

78. Oksanen, J. *et al. vegan: Community Ecology Package*. (2019). Available at https://github.com/vegandevs/vegan

79. Harmon, L. J. Tempo and mode of evolutionary radiation in iguanian lizards. *Science* **301**, 961–964 (2003).

80. Harmon, L. J., Weir, J. T., Brock, C. D., Glor, R. E. & Challenger, W. GEIGER: investigating evolutionary radiations. *Bioinformatics* **24**, 129–131 (2008).

81. Matzke, N. J., BioGeoBEARS: BioGeography with Bayesian (and Likelihood) evolutionary analysis in R scripts. R package, version 0.2.1 (2013).